BIO-INSPIRED DELAYED STALL PROPULSOR

W. J. Usab, Jr.
J. Hardin
A. J. Bilanin
Continuum Dynamics, Inc.
34 Lexington Avenue
Ewing, NJ 08618
Bill@Continuum-Dynamics.com

Abstract

This paper provides an overview of the development of a bio-inspired delay stall propulsor (BDSP) concept which employs delayed stall unsteady lift enhancement to increase the lift on propeller blades without adding any complexity to the propulsor. This BDSP concept can provide greatly increased propeller thrust for a given propeller diameter leading to both increased speed and/or maneuverability. Alternately, this technology offers reduced radiated noise while maintaining current thrust levels through both reduction in propulsor rotation speed and acoustic cancellation. Preliminary 2D simulations demonstrating concept feasibility have shown at least a 36% reduction in rotational speed at constant thrust and at least an estimated 4 db reduction in the total radiated acoustic power. It is believed that the BDSP concept will be simple to manufacture, rugged, and easy to retrofit into existing designs. This technology has direct application to torpedoes, unmanned underwater vehicles (UUVs), maneuvering thrusters, submarines, and other propeller driven devices.

Introduction

Current generation propulsor designs have been optimized using steady flow design concepts and tools. Major advances in propulsor performance, especially with regard to increasing thrust and reducing rotational speeds (and radiated noise), must come from innovative technologies which move beyond the current "steady flow" design space. The new frontier lies in the design of systems which harness and exploit unsteady phenomena. Recent research in biological motion of insects (the fruit fly) has identified three new unsteady lift enhancement mechanisms used by insects: delayed stall, rotational lift, and vortex capture. With these unsteady mechanisms insects generate lift and maneuvering forces which far exceed levels possible under steady flow conditions.

Over the past 5+ years the Naval Undersea Warfare Center (NUWC) Division has been performing groundbreaking work in the development of new biologically inspired maneuvering concepts and high thrust/low noise propulsor concepts. NUWC has focused on distilling the fundamental fluid dynamic mechanisms found in nature and then incorporating them into Navy maneuvering and propulsion systems (see overview by Bandyopadhyay[1]). NUWC has shown that high side-force levels for increased maneuverability can be generated using an actively cambered dorsal fin type control surface[2], and the generation of high thrust/side forces with several flapping foil test models (Bandyopadhyay et al.[3]).

NUWC is also leading the way in the development of biomimetic propulsor concepts for active noise control with the application of electro-active polymeric artificial muscles in the design of programmable cambering blades (actively cambered blades). It was observed in a modeling study that a reduction in rotation rate of the propulsor leads to a reduction in the sources of radiated noise, which include blade tonal due to wake deficit; trailing edge singing; and ingested turbulence.[4] These noise sources were shown to be a function of rotational rate to the power of 4, 5, and 6, respectively. Bandyopadhyay et al.[4] have designed and tested a propeller with actively cambered blades. Oscillatory cambering of the propeller blades was shown to yield a 15% increase in average thrust. From this it was inferred that oscillatory cambering of propeller blades would allow a 7% reduction RPM at constant thrust leading to a little more than the 3-5 dB noise reduction suggested above.

The recent research in biological lift enhancement mechanisms in combination with the NUWC research into the application of these concepts for propulsor thrust enhancement and acoustic signature reduction provided the inspiration for the development of a new bio-inspired delayed stall propulsor (BDSP) concept presented here. The key innovation in the present concept lies in the incorporation of delayed stall lift enhancement into the propulsor in a purely passive (non-actuated) manner. The BDSP concept offers both the potential for increased thrust, as well as, reductions in the far field propulsor noise through a reduction in RPM if the thrust is held constant. Further as this project has progressed, it has become increasingly clear that this delayed stall thrust enhancement concept has promising applications to a broader range of other rotating devices including fans, compressors, pumps, and etc.

Delayed Stall in Insect Flight

Recent theoretical and experimental research (Ellington [6] and Dickinson et al. [7]) has identified three distinct unsteady lift enhancement mechanisms used by insects: delayed stall associated with translational wing motion; rotational lift associated with rotational wing motion (pronation and supination); and wake capture, also associated with rotational wing motion. Tremendous leaps in performance and maneuverability are possible if we can effectively incorporate these unsteady lift enhancement mechanisms in our vehicle designs. Of these, delayed stall holds the most promise for increasing performance of propeller propulsion systems, since in a rotational reference frame the propeller flow can be viewed as undergoing translational motion, and it can be implemented without the need for any type of active surfaces.

Past work by Francis and Cohen [8] showed that an impulsively started wing at large incidences (above the steady state stall limit) travels several chord lengths before the separation associated with stall begins. During this period the wing experiences large transient lift forces. Francis and Cohen [8] measured lift forces greater than the steady stall limit value after only 1.5 chords of travel, with peak lift values exceeding the steady stall limit value by 40-50% when stall finally occurred. These transient lift forces are the result of the translational lift enhancement mechanism called delayed stall.

More recently, studies using real and dynamically scaled models of hawk moths

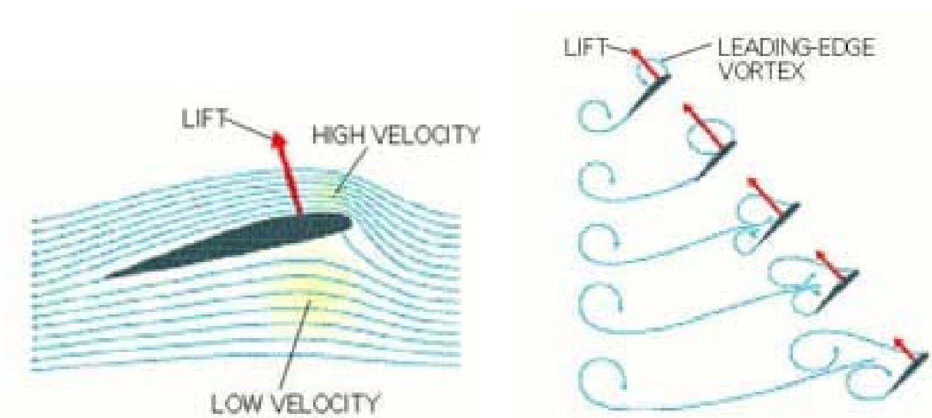

Figure 1: An aircraft wing generates lift by steady-flow aerodynamics (*left*). If the angle of attack is too great (*right*), the wing stalls. When a stall begins, a leading-edge vortex forms with a high flow velocity that momentarily increases lift. The vortex quickly detaches from the wing, however, and greatly reduces lift (figure taken from Dickinson [5]).

(Ellington [6] and Dickinson et al. [7]) have suggested that delayed stall might explain how insect wings generate such large forces. As Dickinson's experiments have shown, insect wings do not stall instantly; rather, it takes some time for the lift-generating flow to break down as the wing angle of attack increases. During the initial stages of the stall process, the lift can greatly exceed the steady stall limit lift due to the formation of a leading-edge vortex located above and behind the wing's leading edge (Figure 1). The key to insects maintaining high lift levels lies in the rapid flapping motion which reverses the wing motion at the point where the vortex separates from the leading edge, essentially starting the delayed stall process in the opposite direction and preventing a large reduction in lift.

Bio-inspired Delayed Stall Propulsor Concept

The unsteady delayed stall lift enhancement mechanism can be incorporated into a propeller for increased thrust in the following passive manner. First, it may be observed that in a reference frame rotating with a propeller, each propeller blade can be viewed as undergoing steady translational motion in the circumferential direction. For the present discussion we consider unrolling a constant radius circumferential cut through a propeller, resulting in an infinite cascade of blades. Under steady conditions with uniform axial inflow, the local flow incidence for each blade would be constant in time (a function of on-coming flow speed and direction, the propeller rotational speed, and radial location).

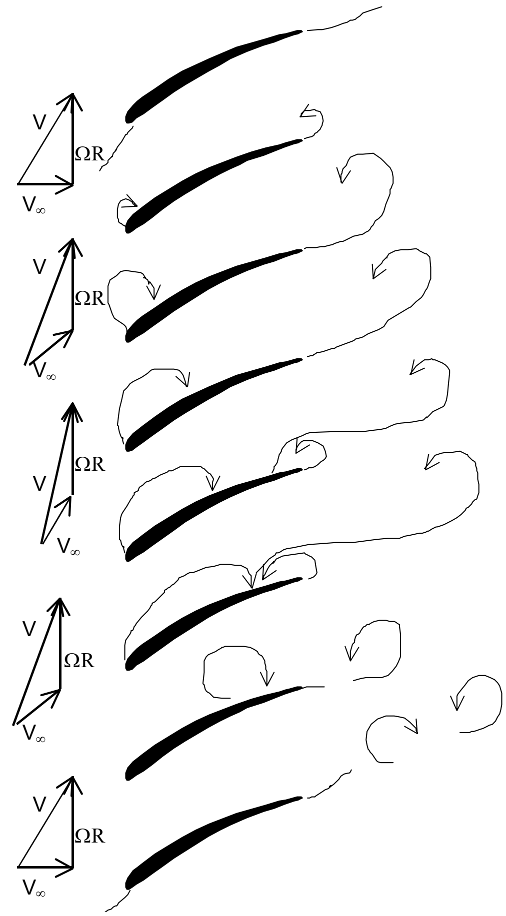

Figure 2 Propeller cascade with circumferentially periodic variation in the inflow velocity, V_∞.

Now imagine the introduction of a circumferentially periodic variation in the onset flow to this cascade of blades as shown in Figure 2. With proper selection of the onset flow variation period, flow magnitude, and direction, one can envision the situation where each blade undergoes a periodic cycling of the local flow incidence above the steady stall incidence, resulting in periodic delayed stall lift enhancement. Each blade then cycles between stall onset with very high blade sectional lift coefficients and the formation of a leading edge vortex, and flow reattachment at lower blade incidences where the leading edge vortex detaches and convects downstream. Figure 3 illustrates the anticipated behavior of the unsteady lift force. This behavior is at the heart of the innovation proposed here.

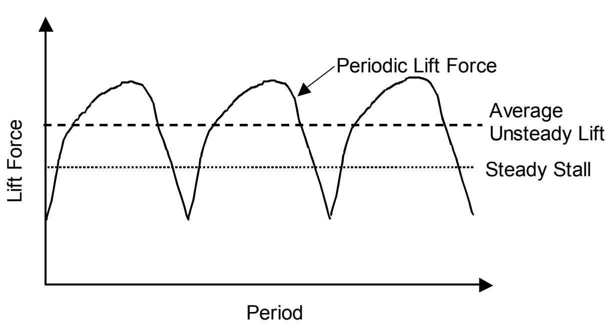

Figure 3 Periodic and average lift force on wing undergoing oscillating delayed stall motion.

Since the propeller is rotating, there are many ways to introduce the required periodic variation in blade incidence. The approach taken here is to place a stator blade row upstream of the propeller, with a circumferentially (and potentially radial) variation in the stator blade geometries between adjoining blades. For ducted propeller configurations this stator blade row could be integrated with the propeller support struts.

An alternate approach is to consider a counter-rotating propeller configuration where a circumferential variation in the blade geometry is designed into the upstream propeller to drive the cyclic delayed stall lift enhancement on the second propeller blade row. This latter approach may have advantages if higher frequency periodic disturbances are required. Further, if the two propeller blade rows are placed close together, it may be possible to use the second propeller blade row to introduce upstream propagating periodic disturbances, which will allow incorporation of the same delayed stall lift enhancement mechanism on the upstream propeller.

Symmetry Constraints for Constant Total Thrust

While increasing thrust is of great interest, for many propulsor applications, it is also important that net thrust not have a significant unsteady component (for example to minimize vibration and fatigue in drive system components or for passenger comfort). Minimization of the unsteady component of the net thrust is of particular interest in acoustic signature reduction, since unsteady forcing from the propulsor can turn the vehicle into a large acoustic radiator.

If properly designed and matched to the propeller, the introduction of a circumferential inflow variation would place each propeller blade into a delayed stall cycle leading to high levels of average thrust. By introducing special symmetries into both the circumferential inflow profiles and the number of propeller blades used, one can minimize the net unsteady loading on the propeller.

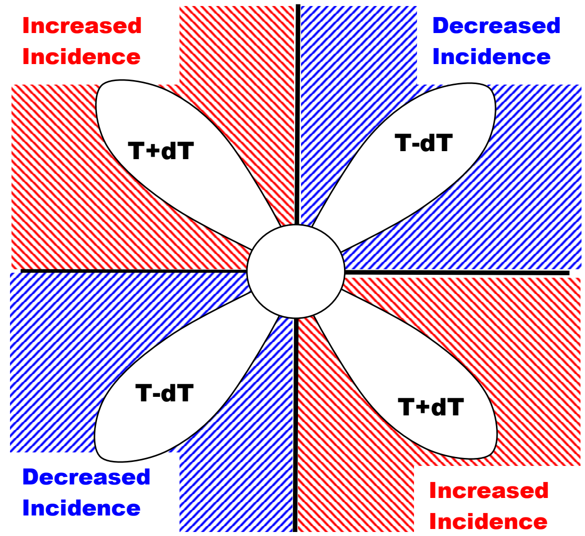

Figure 4: Example four bladed propeller undergoing two cycles of incidence variation per propeller revolution (N=2).

For example, consider the four bladed propeller shown in Figure 4 and assume it has a stator (not shown) that increases the flow incidence (increased swirl) which each propeller sees in the first and third quadrants and decreases the flow incidence (decreased swirl) in the second and forth quadrants. Then each propeller blade would undergo two delayed stall cycles per propeller revolution with periodically varying thrust. A cascade view of the same configuration is shown in Figure 5. From this prospective it becomes clear that at any given instant in time two blades will have thrust forces of **¼T+dT** where **T** is the average thrust and **dT** is the unsteady component, and two blades will have a thrust force **¼T-dT**. Because of the tailoring of the periodic inflow swirl profile the net force for the four blades will always be **T**. Further, the unsteady loading symmetry will cancel moments on this propeller.

Hence, while each blade is undergoing a cyclic variation of the loading at a frequency, which is twice the rotational speed, the total thrust will be constant (or nearly constant) and much higher than possible without the incorporation of this delayed stall phenomena. Finally, introduction of this type of symmetry also leads to acoustic cancellation in the far field.

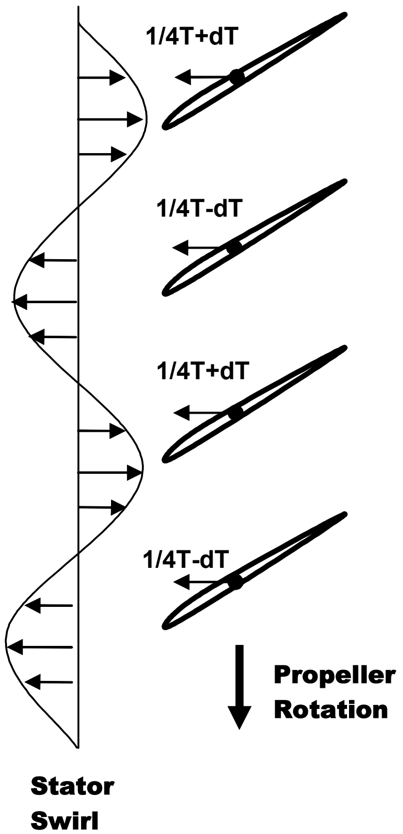

Figure 5 Cascade view of four bladed propeller undergoing two cycles of incidence variation per propeller revolution.

In general, uniform total thrust and acoustic cancellation are possible for propeller configurations with 2MJ propeller blades and M cycles in the onset flow per revolution, where M = 2, 3, 4, ... and J = 1, 2, 3, ….

Hydrodynamic BDSP Model

Given this problem complexity, the approach taken here was to formulate a two dimensional simulation of the stator-rotor interaction which included empirically modeled delayed stall effects. This stator-rotor model was then coupled with an optimization algorithm allowing us to vary the stator imposed inflow and selected propeller characteristics to maximize the propeller thrust while minimizing the unsteady component of the total propeller thrust. This section outlines the hydrodynamic model used to demonstrate the potential thrust enhancement possible using the BDSP concept.

The stator-rotor interaction problem was modeled as a two-dimensional cascade as shown in Figure 6. This model comes about by imagining a constant radius cut through the stator-rotor combination and then unrolling it. The stator was then modeled as a row of vortices of varying strengths Γ_i, i=1, …, N_s, which is then repeated infinitely in both directions. The propeller rotor is modeled as a row of N_r blades of the same section profile and stagger angle β, rotating at angular velocity Ω, and R the section radius. The loading on each propeller blade is determined by the combination of a freestream onset flow V_{fs}, the stator row, and an empirical delayed stall model for the propeller (described below).

Given this model, the time dependent loading on each blade can be computed by marching the rotor through one revolution. Due to the lift hysteresis of delayed stall phenomena the solution was marched through two revolutions to capture the periodic response. Then the total time dependent thrust (T), average thrust (T_{ave}), and maximum excursion in the unsteady thrust ($|\Delta T| = |T-T_{ave}|$) were computed based on the second revolution of the stator-rotor system.

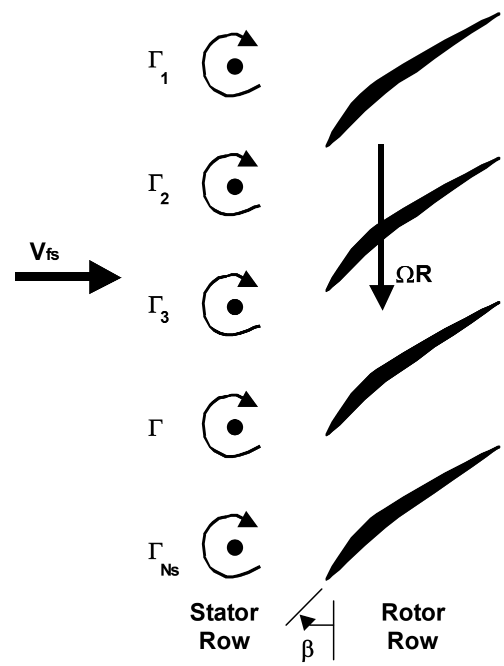

Figure 6 Schematic of stator-rotor interaction model.

The loading of each propeller blade was predicted using the Johnson formulation[9, 10] of the Boeing dynamic stall model[11-13]. Dynamic stall is characterized by a delay in the occurrence of separated flow produced by the wing motion, and high transient loads induced by a vortex shed from the leading edge when stall does occur. In the Johnson formulation 2D steady section force coefficient data for a given airfoil section is used in combination with a delayed angle of attack (α_d) calculated from the local section angle of attack, α. Predicted section force and moment coefficients are defined as follows,

$$c_L = \left(\frac{\alpha - \alpha_z}{\alpha_d - \alpha_z}\right)(c_l)_{2D}\Big|_{\alpha_d} + (c_l)_{US}$$

$$c_D = \left(\frac{\alpha - \alpha_z}{\alpha_d - \alpha_z}\right)^2 \left[(c_d)_{2D}\Big|_{\alpha_d} - c_{dz}\right] + c_{dz} + (c_d)_{US}$$

$$c_M = \left(\frac{\alpha - \alpha_z}{\alpha_d - \alpha_z}\right) \left[(c_m)_{2D}\Big|_{\alpha_d} - c_{mz}\right] + c_{mz} + (c_m)_{US}$$

where α_z is the zero-lift angle of attack, and c_{dz} and c_{mz} are the corresponding drag and moment. $(\,)_{US}$ are the unsteady loads due to pitch rate based on thin airfoil theory. The form of the lift and moment corrections ensures that the coefficients below stall are unchanged. In general the 2D section force coefficient data is provided in tabular form.

The Boeing dynamic stall model[11-13] uses an angle of attack delay proportional to the square-root of $\dot{\alpha}$, which produces the basic hysteresis effects. The delayed angle of attack is given by

$$\alpha_d = \alpha - \tau_d \sqrt{\left|\frac{\dot{\alpha} c}{2U}\right|}\ sign(\dot{\alpha})$$

Alternatively, this can be considered a time lag, which is dependent on the pitch rate. The time constant τ_d is in general a function of Mach number and the airfoil section, obtained from oscillating airfoil tests. All the results presented here used a NACA0012 airfoil section for which τ_d=1.1 based on NASA experimental data.[14]

An in-house optimization routine was used to maximize the total thrust and minimize the unsteady component of the total thrust for a specified free stream velocity (V_{fs}) and propeller rotation speed (Ω). A flow chart for this optimization problem is shown in Figure 7.

Starting with a baseline steady propulsor configuration selected to be representative of torpedo operating conditions; two optimization problems were considered to demonstrate the BDSP concept. In the first, the stator-rotor configuration was optimized to maximize thrust at constant RPM using delayed stall lift enhancement. In the second case, the stator-rotor configuration was optimized to minimize the rotational speed while holding the thrust constant at the baseline configuration level. The latter example indicates the potential noise reduction that can be achieved for those noise sources, which scale with the propulsor rotational speed.

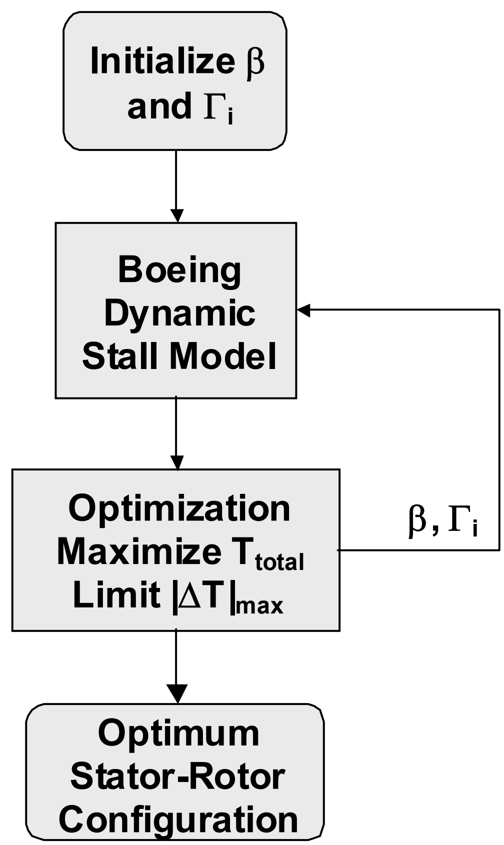

Figure 7 Flow chart of stator-rotor passive delayed stall optimization model.

Table 1 Unofficial published Navy torpedo characteristics

Model	Service Date	Length (ft)	Diameter (ft)	Speed (kts)
MK-46	1965	8.5	1.06	45
MK-48	1972	19.3	1.75	40-55
MK-50	1990	9.5	1.06	50+

Table 2 Baseline propeller configuration

Parameter	Value
V_{fs}	50 kts = 84.4 ft/s
Ω	226 rad/sec
r/R	0.8
D	2.0 ft
C_L design	0.6
β	30.5 degrees

Baseline Torpedo Configuration

A torpedo propulsor was chosen for demonstration purposes as the target platform for the bio-inspired delayed stall propulsor (BDSP) concept. Published characteristics for three current generation Navy torpedoes are summarized in Table 1. Based on this information a generic baseline configuration was constructed with a four bladed propeller operating at 50 kts = 84.4 ft/s and a diameter of two feet. Since there is no published data on rotation speeds for these configurations we chose a propeller rotation speed of 226 rad/sec. A baseline section C_L=0.6, believed to be on the high side, was chosen to be conservative for our estimates. Spanwise location, r/R=0.8, was selected as representative of the total propeller. Given the forward speed, propeller rotation speed, and steady section loading leads to a rotor stagger angle of β=30.5 degrees. The complete baseline configuration is summarized in Table 2.

Using the 2D stator-rotor interaction analysis without a cascade blade row, the total steady thrust and torque for this configuration was computed. For clarity and convenience all BDSP configuration results have been normalized by the results from this baseline configuration.

BDSP Thrust Optimization at constant RPM

The first bio-inspired delayed stall propulsor configuration was optimized for maximum total thrust, T, while minimizing the peak unsteady total thrust variation, defined as $|\Delta T|_{max} = |T(t)-T_{ave}|$. Figure 8 presents the normalized thrust as a function of time for the optimized configuration. All thrust values are normalized by the baseline thrust, $T_{baseline}$. The lower curves in this figure show the unsteady thrust loading for each of the four blades. Due to the symmetry designed into this device, blades 0 and 2 and blades 1 and 3 see exactly the same loading, thus canceling moments on the propeller over each propeller revolution. Note that each blade goes through two dynamic stall cycles per revolution. The optimized bio-inspired delayed stall propulsor has an average thrust which is 2.2 times the baseline thrust, as shown by the constant upper line in Figure 8.

The oscillatory upper line in this figure is the total time dependent thrust. Note that by taking advantage of the symmetry of this four bladed design, with optimization of the stator to minimize the unsteady component of the total thrust, the peak excursions from the average thrust values are 7% of the average thrust level. It is believed, but has not been shown here, that this excursion can be eliminated by further refinement of the periodic incident flow field. Given the approximate nature of this analysis model, further refinement would have little engineering value.

The section lift coefficient vs. local flow incidence for blade 0 is presented in Figure 9. This hysteresis loop is typical of an airfoil undergoing dynamic stall. Note that the local flow incidence to the blade cycles between about 10 degrees and 28 degrees as measured from the section chord line. Peak section lift coefficient values are above 2.5, which is well beyond the steady stall limit of about 1.2, and only possible through dynamic stall lift enhancement.

Speed Optimization at Constant Thrust

One of the important objectives of this research effort was to demonstrate the feasibility of using delayed stall phenomena to attain the same thrust at a lower propeller rotational speed

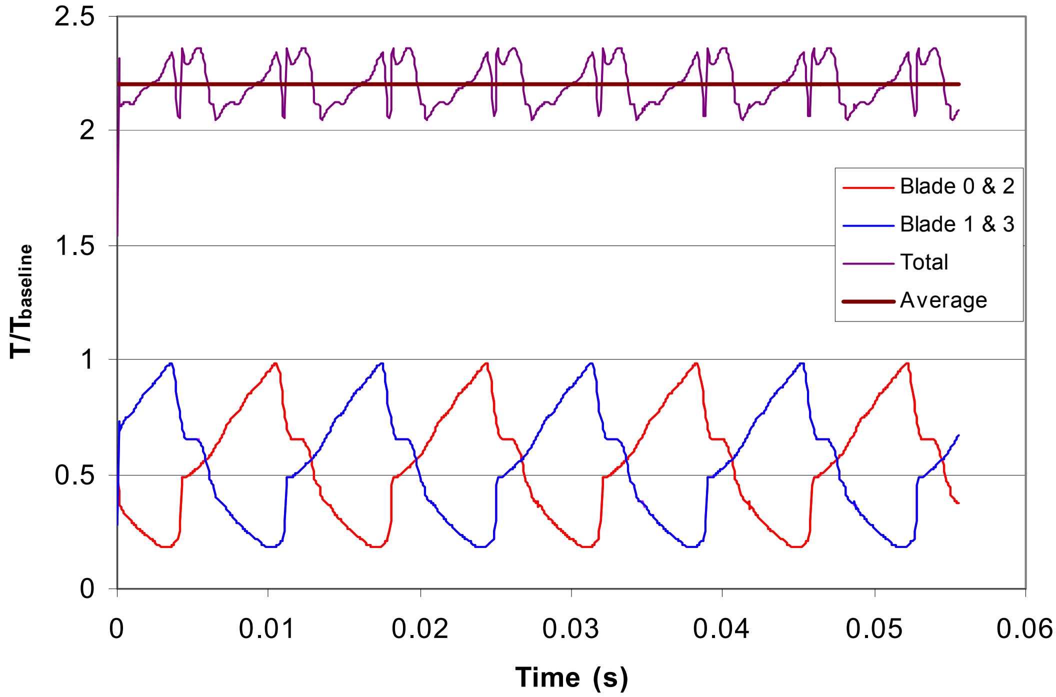

Figure 8 Optimized BDSP configuration at constant RPM: Thrust vs. Time.

leading to a decrease in the total radiated acoustic power. Starting with the thrust optimized design configuration in the previous section, a series of thrust optimization calculations were performed at lower and lower propeller rotation speeds. The rotational speed was reduced until the predicted optimized thrust matched the baseline thrust level.

The thrust and section lift coefficient as a function of time for the rotational speed optimized BDSP configuration is presented in Figure 10. The propeller rotation speed for the optimized constant thrust BDSP configuration was determined to be approximately 144 rad/sec. This result is a 36% decrease in rotation speed over the baseline configuration, with the same thrust. Based on the preliminary acoustic analysis which follows, this 36% reduction in RPM with this four bladed configuration, will yield a 4 db reduction in the radiated sound power over the baseline configuration.

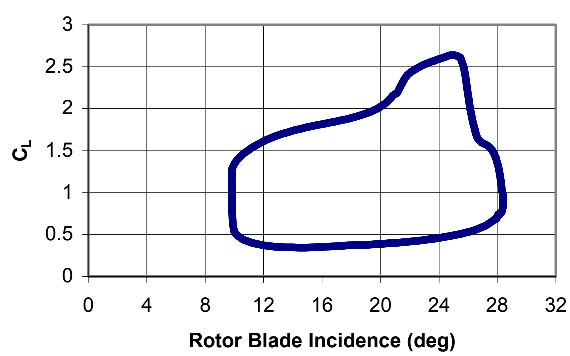

Figure 9 Optimized BDSP configuration at constant RPM: Section C_L as a function of rotor blade incidence.

Acoustic Scaling for an Isolated Propeller with Periodic Inflow

The sources of radiated noise for a propulsor are blade tonals due to the unsteady lift on the propeller blades resulting from circumferential variation in the inflow to the propeller (including wake deficits), tailing edge singing, turbulence ingestion, and cavitation. As discussed in

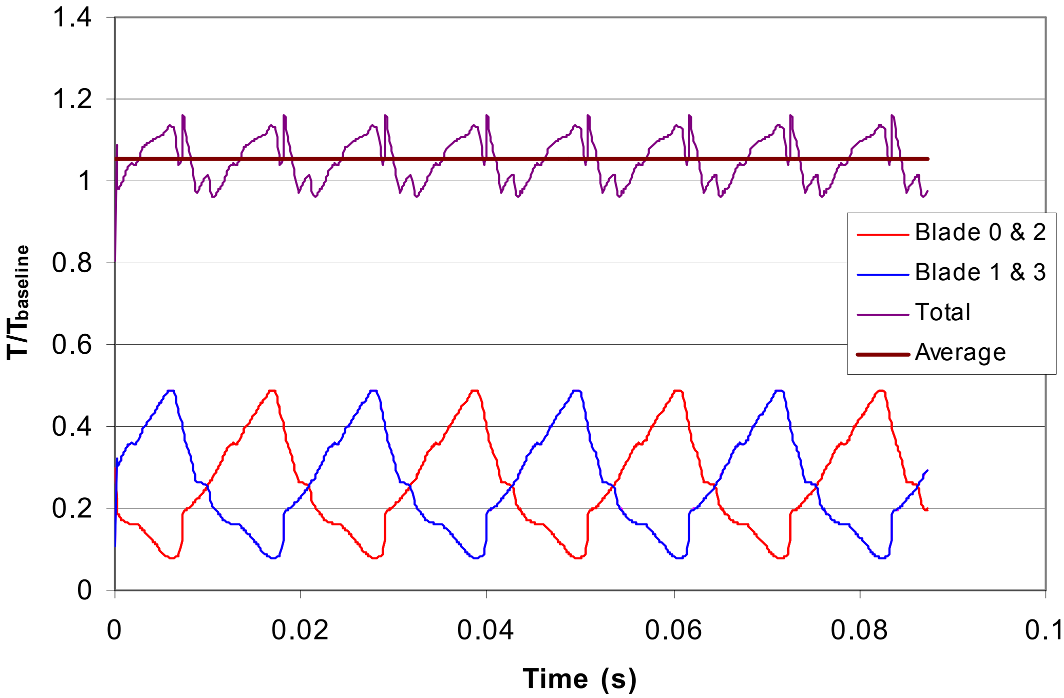

Figure 10 Optimized BDSP configuration at constant thrust: Thrust vs. Time.

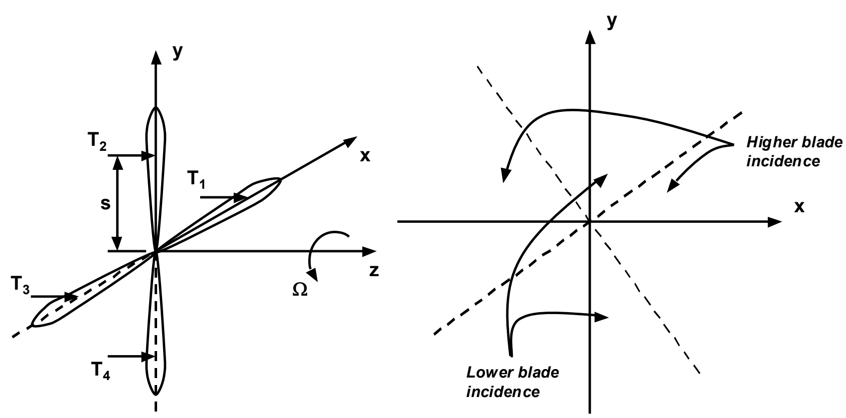

Figure 11 Four bladed propeller (left) and stator induced incidence variation on rotor (right).

Ross[15] and summarized in Bandyopadhyay, et al.[4], trailing edge singing and turbulence ingestion scale as 5^{th} and 6^{th} powers of propeller rotation speed, Ω, respectively. The blade rate tonals scale as the 2^{nd} power of Ω if the thrust is held constant, making it the dominate noise source with reducing RPM. Based on these scaling laws, we focused the acoustic analysis on an assessment of potential penalties associated with the introduction of unsteady lift on the propeller blades (i.e., blade tonal noise).

Assume a four-bladed propeller with the thrust on each blade acting at an effective radius, s, and modulating as $T_i(t)$ due to the local flow incidence variation from quadrant to quadrant as shown in Figure 11 (Left). To an observer at a great distance from the propeller the four blades may be replaced by 4 rotating dipoles.

The acoustic pressure radiated to observer is given by

$$4\pi p(\bar{x},t) = -\frac{\partial}{\partial z}\sum_{n=1}^{4}\frac{T_n(t - r_n / c)}{r_n}$$

where assuming two cycles/rev

$$T_n(t) = \bar{T}\cos[4\Omega t] + \Delta T\cos 2\theta\cos[4\Omega t - (n-1)\pi/2]$$

$$\bar{T}_n = \bar{T} = const,\ n = 1-4, \quad \Omega = blade\ rotation\ rate$$

$$r_1 = [(x-s)^2 + y^2 + z^2)]^{1/2}\ etc.$$

Here $\bar{T}$ is the mean thrust produced by a blade and ΔT is the maximum fluctuation in the thrust, the $\cos(2\theta)$ term, where $\theta = \Omega t$, accounts for the fact that the thrust varies twice per revolution and that the maximum and minimum thrust values always occur at the same locations in θ while 4Ω is the blade passage frequency.

Expanding the expression for the acoustic pressure in a Taylor series about the origin, assuming an acoustically compact radiating sound source, squaring the pressure, and integrating over a large spherical surface leads to an expression for the total sound power radiated which is proportional to a dipole and quadrapole terms:

$$P \propto \frac{4\pi}{3}(128)\,\Omega^2\bar{T}^2 + \frac{8\pi}{15}\,\frac{(656)\Omega^4 s^2(\Delta T)}{c^2}$$

where c is the speed of sound. In this expression, the left term is a dipole and the right is a quadrapole.

Consider a typical torpedo application with s = 1 ft, Ω = 226 rad/sec, c = 5000 ft/sec for water, and assume ΔT/T ~ O(1). Then the dipole contribution is $O(10^4)$ larger than the quadrapole term or the sound power radiated by the dipole is 40 db higher than that of the quadrapole. Therefore the quadrapole term is negligible relative to the dipole noise, which is a direct consequence of the load symmetry designed into this configuration (i.e., 4 bladed propeller with two delay stall cycles per propeller revolution).

It is well known that the thrust is proportional to Ω^2 and can be approximated by

$$\bar{T} \propto C_L Nsc\frac{1}{2}\rho s^2\Omega^2$$

where N is the number of blades, c is the blade chord, ρ is the fluid density, and C_L is the lift coefficient for the blade . Then the acoustic power from the dipole scales as Ω^6, assuming C_L = constant. It is important to note that this scaling does not hold for constant thrust. As shown in the expression for total sound power radiated, if the thrust is held constant then the dipole term, and hence radiated acoustic power, scales as Ω^2.

Consider a baseline steady thrust configuration with thrust $T_{baseline}$ and rotational speed $\Omega_{baseline}$, and a new bio-inspired delayed stall configuration with average thrust T_{DS} and rotational speed Ω_{DS}. Now assume that the delayed stall configuration has the same thrust as the baseline configuration, but with lower rotational speed due to the higher blade loading possible with the delayed stall phenomena. Then the reduction in total sound power is given by

$$db\ \text{Re}\,duction = 10\,\log\left[\frac{P_{DS}}{P_{baseline}}\right] = 10\,\log\left[\frac{(\bar{T}\Omega)^2_{DS}}{(\bar{T}\Omega)^2_{baseline}}\right] = 10\,\log\left[\frac{\Omega^2_{DS}}{\Omega^2_{baseline}}\right]$$

Based on this expression, Figure 13 estimates the sound power reduction at constant thrust which can be attained by reducing the propeller rotation speed. For example, in the current case a reduction of 36% in rotation speed ($\underline{\Omega_{baseline}}/\underline{\Omega_{DS}}$ = 1.57) corresponds to a predicted farfield sound power reduction of 4 db.

Delayed Stall Fan Test

There are a wide range of potential applications of delayed stall lift enhancement technology in the development of new air handling systems fans (heating, air-conditioning,

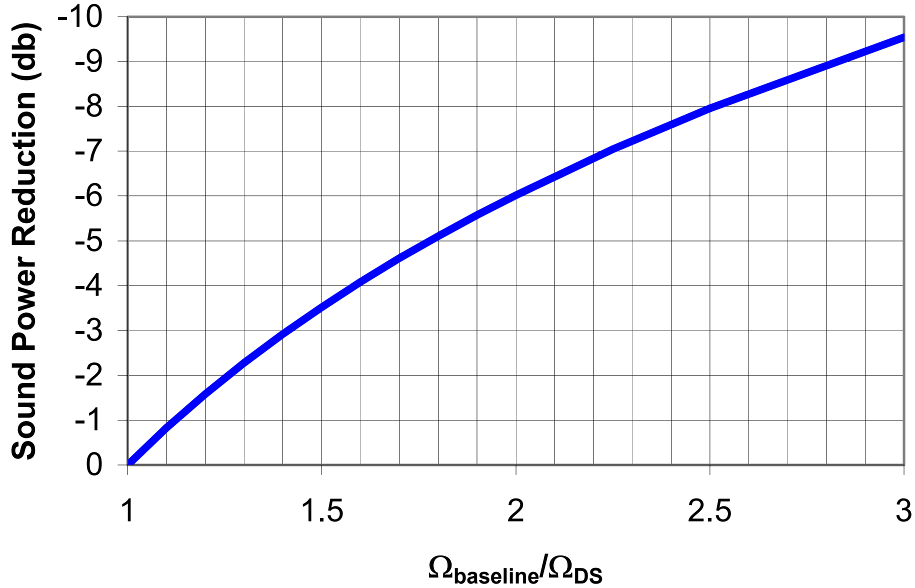

Figure 13: Estimated sound power reduction as a function of increased lift coefficient at constant thrust.

and ventilation systems). Since these systems run around the clock for both heating and cooling, even modest performance gains can have a major cost advantage over the life of the system.

A special 22" diameter delayed stall fan technology demonstrator was design and

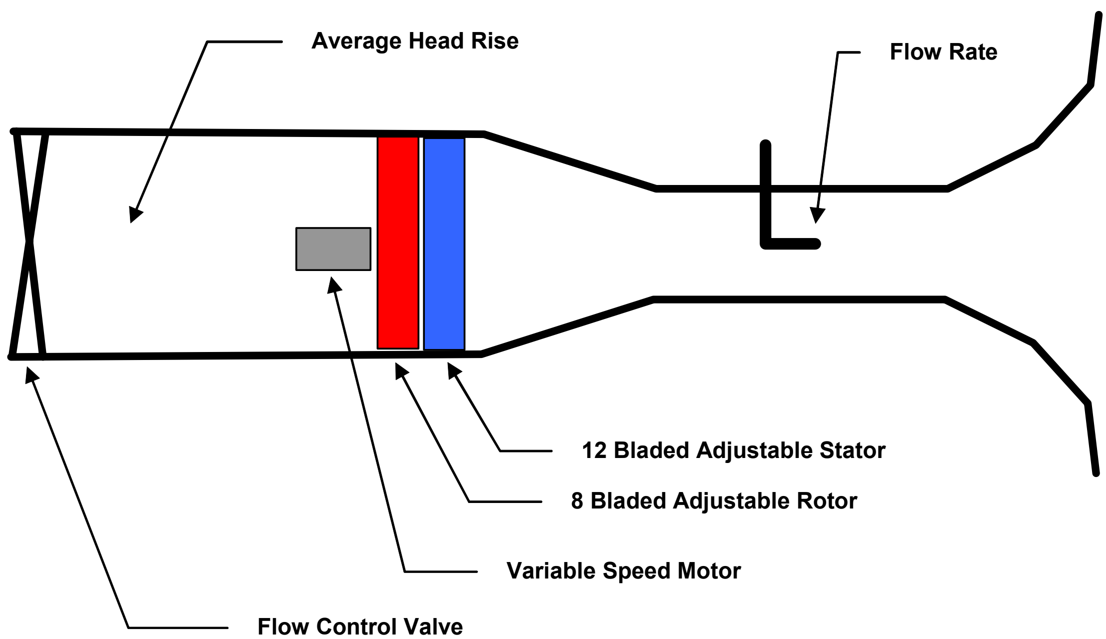

Figure 12 Delayed stall fan test facility schematic.

Figure 14: CDI's delayed stall fan rig: eight bladed rotor (left) and 12 bladed adjustable stator assembly (right).

installed in our low speed wind tunnel diffuser section. This delayed stall fan test rig is shown schematically in Figure 12. The fan (or rotor) is constructed of eight untwisted blades, each set at the same pitch angle (Figure 14 left). In front of this fan rotor is a stator assembly composed of 12 stator blades (Figure 14 right). Both stator and rotor blades were constructed with NACA0006 sections, a 4" chord, and 8" span. The pitch of each stator blade can be individually set, allowing the generation of different circumferential varying swirl patterns which induce the cyclic delayed stall lift enhancement on the following fan rotor.

Mass flow and upstream total pressure measurements were made using the pitot static probe located in the wind tunnel test section upstream of the fan (see Figure 12). Average total pressure measurements were made 2.5 rotor diameters downstream of the fan using 6 total pressure probes distributed circumferentially at the 75% radial location measured from the rotor centerline. A louvered gate was placed 6 rotor diameters downstream to control the mass flow through the test rig.

To illustrate the potential performance benefits of incorporation of delayed stall, consider the following baseline and delayed stall fan configurations. For the baseline configuration the stator blades were set to be aligned with the axial flow direction (no stator induced swirl).

Two delayed stall configuration where constructed where the stator blade pitch angles were varied circumferentially to induce two cycles of the delayed stall phenomena for each fan blade revolution. In the first delayed stall configuration the stator pitch angles were varied in the range of 0 to 30 degrees with the following blade setting angles going clockwise around the stator faces: 0, 0, 15, 30, 30, 15, 0, 0, 15, 30, 30, and 15 degrees. Figure 14 (right) shows the stator assembly in this delayed stall configuration. In the second the maximum pitch angle was increased to 40 degrees with the following stator pitch angle sequence: 0, 0, 20, 40, 40, 20, 0, 0, 20, 40, 40, and 20 degrees.

Constant rotational speed tests were run for each configuration while varying the mass flow through the stage using the louver gate. Measurements were made of the mass flow through the fan stage and the total pressure rise across the fan stage (essentially, back pressuring the fan). Figure 15 presents Ω = 1125 RPM constant fan speed curves for the baseline and two delayed stall configurations showing the

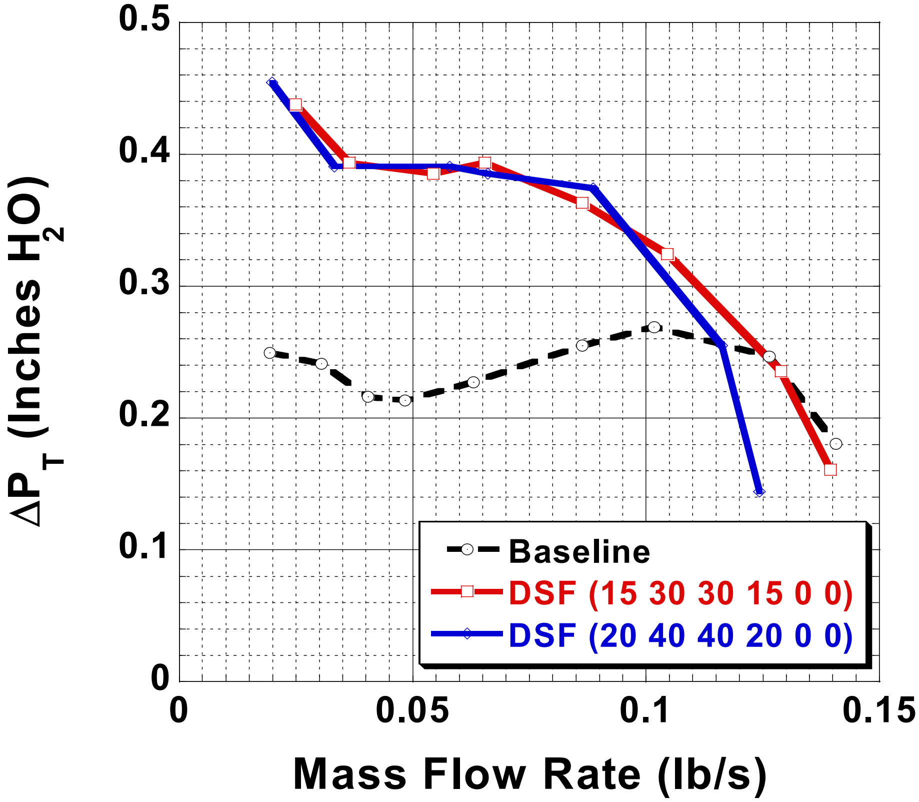

Figure 15: Comparison of baseline and delayed stall fan configurations showing total pressure rise across the fan stage with mass flow rate at constant fan rotation speed (Ω = 1125 RPM).

total pressure rise across the stage as a function of mass flow rate.

As the fan stage is back pressured, the total pressure rise across the fan increases while the mass flow rate through the fan decreases. This process will continue until the fan stalls, as shown by the baseline curve in Figure 15. Observe that, as the mass flow is further reduced, the total pressure rise reaches a peak then flattens off at a lower level. This is an indication that the fan blades are undergoing a steady stall condition. Further back pressuring of the fan (or reduction in mass flow rate) has very little influence on the total pressure rise since the flow over the fan blades has stalled.

In contrast, incorporating delayed stall lift enhancement into this fan configuration results in a increase in the total pressure rise across the fan stage. As shown in Figure 15, relative to the baseline configuration, the increase in total pressure rise reaches a maximum level 50% higher than the baseline configuration in the lower mass flow range. Note that at the high mass flow range, the delayed stall configuration curves cross the baseline configuration curve. In this range the blades are lightly loaded and below the delayed stall enhancement range. It is important to note that the delayed stall lift enhancement effect is significant over a broad operating range. Further, the delayed stall configurations do not exhibit the classical drop off in the total pressure recovery at low mass flow rates, thus providing a much larger stall margin.

Comparing the two delayed stall configurations, it can be observed from Figure 15 that both the 30 deg. and 40 deg. stator pitch cycles result in the same increases in the total pressure rise in the low mass flow regime. Outside the delayed stall regime, the 30 deg. configuration performs better than the larger pitch cycle 40 deg. configuration. One would expect that there would be higher losses associated with the large pitch variation around the stator when operating the fan in a regime where the blades are lightly loaded.

While no effort has been made to optimize the delayed stall phenomena in the present delayed stall fan configurations, these preliminary results clearly illustrate that incorporation of delayed stall lift enhancement into a compressor system offers the potential for increased performance (i.e., increased total pressure rise across each stage) and increased stall margin. Increasing the performance per stage means that new compressors can be designed with fewer stages or fewer blades for the same system pressure ratio, leading to an overall reduction in system costs and part counts.

Conclusions

The overall objective of the present work was to develop and demonstrate the feasibility a bio-inspired delayed stall propulsor that uses the delayed stall mechanism to provide propeller thrust coefficients which greatly exceed current steady flow stall limits. The fundamental idea suggested here is that delayed stall lift enhancement can be incorporated into a propeller design through the introduction of a circumferential variation in the propeller onset flow. The BDSP concept enhances thrust by harnessing and optimizing the dynamic stall process in a fixed geometry stator-rotor configuration.

There are many advantages of the “passive” concept as envisioned here. First, the delayed stall lift enhancement mechanism is introduced in a way that takes advantage of the rotating propeller environment and, special symmetry between the stator induced flow and the propeller. This approach does not require any on-blade actuation devices to obtain the necessary cyclic variation in the local blade incidences. In fact, it is completely passive. This feature minimizes both the mechanical complexity and the development/fabrication costs.

Preliminary 2D simulations have demonstrated a factor of two or more increase in thrust is possible at constant RPM. Further this thrust enhancement was obtained while minimizing the unsteady component of the thrust. As shown, the natural symmetry of the BDSP design leads to nearly constant total thrust, even though there is cyclic loading in individual blades. Further, these symmetries lead to far field cancellation of the radiated sound power from the unsteady loading of individual blades.

Increasing the obtainable propeller thrust coefficient using the delayed stall lift enhancement also offers the potential for reducing sound radiation, since for the same thrust as a conventional propeller configuration, this new design can operate at a much lower rotational speed due to the much higher blade loadings (propeller advance ratio). Model simulations demonstrated a 36%+ reduction in rotational speed at constant thrust. Preliminary acoustic analysis of the BDSP estimates a 4 db to 8.6 db reduction on total radiated acoustic power as a direct result of the lowering of the propeller rotational speed (depending on the blade loading of the baseline configuration).

The lift enhancement technology being developed here has much broader application industrial pumps, compressors, and fans. Preliminary testing has demonstrated increased stall margins and up to a 50% increase in total pressure rise across fans at low mass flow rates when using delayed stall lift enhancement.

Acknowledgements

Portions of this work were sponsored by ONR through the Navy Small Business Innovative Research Program (Contract N00014-02-M-0210, TPOC: Dr. Promode Bandyopadhay). Dr. Bandyopadahay’s support, guidance, and technical feedback during the course of this project are greatly appreciated. Continuum Dynamics, Inc. sponsored the development of the delayed stall fan facility and delayed stall fan test program.

References

[1] P. Bandyopadhyay, "Maneuvering Hydrodynamics of Fish and Small

Underwater Vehicles," *Integrative and Comparative Biology*, vol. 42, pp. 102-117, 2002.

[2] P. Bandyopadhyay, J. M. Castano, J. Q. Rice, R. B. Phillips, W. H. Nedderman, and W. K. Macy, "Low-speed Maneuvering Hydrodynamics of Fish and Small Underwater Vehicles," *ASME Journal of Fluids Engineering*, vol. 119, pp. 136-143, 1997.

[3] P. Bandyopadhyay, J. M. Castano, W. H. Nedderman, and M. J. Donnelly, "Experimental Simulation of Fish-inspired Unsteady Vortex Dynamics on a Rigid Cylinder," *ASME Journal of Fluids Engineering*, vol. 122, pp. 219-238, 2000.

[4] P. Bandyopadhyay, J. Krol, William P., D. P. Thivierge, W. H. Nedderman, and M. Mojarrad, "A Biomimetic Propulsor for Active Noise Control: Experiments," Naval Undersea Warfare Center Division, Newport, RI, NUWC-NPT Technical Report 11,351, March 2002.

[5] M. Dickinson, "Solving the Mystery of Insect Flight," in *Scientific American*, 2001.

[6] C. P. Ellington, "The Aerodynamics of Hovering Insect Flight. IV. Aerodynamic Mechanisms," *Philosophical Transactions of the Royal Society of London. Series B, Biological Sciences*, vol. 305, pp. 79-113, 1984.

[7] M. H. Dickinson, F.-O. Lehmann, and S. P. Sane, "Wing Rotation and the Aerodynamic Basis of Flight," *Science*, vol. 284, pp. 1954-1960, 1999.

[8] R. H. Francis and J. Cohen, "The Flow Near a Wing Which Starts Suddenly from Rest and Then Stalls," *Rep. Memo. Aeronaut. Res. Comm.*, 1933.

[9] W. Johnson, "Rotorcraft Aerodynamics Models for a Comprehensive Analysis," presented at American Helicopter Society 54th Annual Forum, Washington, DC, 1998.

[10] K. Nguyen and W. Johnson, "Evaluation of Dynamic Stall Models with UH-60A Airloads Flight Test Data," presented at American Helicopter Society 54th Annual Forum, Washington, DC, 1998.

[11] F. D. Harris, F. J. Tarzanin, Jr., and R. K. Fisher, Jr., "Rotor High Speed Performance, Theory vs. Test," *Journal of the American Helicopter Society*, vol. 15, pp. 35-44, 1970.

[12] F. Tarzanin, "Prediction of Control Loads Due to Blade Stall," *Journal of AHS*, vol. 17, pp. 33-46, 1972.

[13] R. E. Gormont, "A Mathematical Model of Unsteady Aerodynamics and Radial Flow for Application to Helicopter Rotors," USAAVLABS TR 72-67, May 1973.

[14] K. W. McAlister, W. J. Pucci, W. J. McCroskey, and L. W. Carr, "An Experimental Study of Dynamic Stall on Advanced Airfoil Sections; Volume 2: Pressure and Force Data," NASA TM-84245, September 1982.

[15] D. Ross, *Mechanics of Underwater Noise*. Los Altos, CA: Peninsula Publishing, 1987.